HHS Public Access

Author manuscript

Dev Dyn. Author manuscript; available in PMC 2022 June 05.

Published in final edited form as:

Dev Dyn. 2022 June ; 251(6): 988–1003. doi:10.1002/dvdy.340.

Distinct TLR signaling in the salamander response to tissue damage

Ryan J Debuque[1], **Sergej Nowoshilow**[2], **Katya E Chan**, **Nadia A Rosenthal**[3], **James W Godwin**[1,3,4,*]

[1.]Australian Regenerative Medicine Institute (ARMI), Monash University, Melbourne Victoria. Australia

[2.]The Research Institute of Molecular Pathology (IMP), Vienna. Austria

[3.]The Jackson Laboratory, Bar Harbour, Maine, USA

[4.]The MDI Biological Laboratory (MDIBL), Salisbury Cove, Maine, USA

Abstract

Background: Efficient wound healing or pathogen clearance both rely on balanced inflammatory responses. Inflammation is essential for effective innate immune-cell recruitment; however, excessive inflammation will result in local tissue destruction, pathogen egress, and ineffective pathogen clearance. Sterile and non-sterile inflammation operate with competing functional priorities but share common receptors and overlapping signal transduction pathways. In regenerative organisms such as the salamander, whole limbs can be replaced after amputation while exposed to a non-sterile environment. In mammals, exposure to sterile-injury Damage Associated Molecular Patterns (DAMPS) alters innate immune-cell responsiveness to secondary Pathogen Associated Molecular Pattern (PAMP) exposure.

Results: Using new phospho-flow cytometry techniques to measure signaling in individual cell subsets we compared mouse to salamander inflammation. These studies demonstrated evolutionarily conserved responses to PAMP ligands through Toll-Like Receptors (TLRs) but identified key differences in response to DAMP ligands. Co-exposure of macrophages to DAMPs/PAMPs suppressed MAPK signaling in mammals, but not salamanders, which activate sustained MAPK stimulation in the presence of endogenous DAMPS.

Conclusions: These results reveal an alternative signal transduction network compatible with regeneration that may ultimately lead to the promotion of enhanced tissue repair in mammals.

Graphical Abstract

[*]James W. Godwin (corresponding author: jgodwin@mdibl.org.

Author contributions

Ryan Debuque: Conceptualization Investigation; methodology; analysis; writing and editing.
Sergej Nowoshilow: Resources; Investigation: Provision of Axolotl TLR4 cDNA/protein sequences.
Katya Chan: Investigation; methodology.
Nadia Rosenthal: Funding acquisition; and editing.
James W Godwin: Conceptualization; formal analysis; funding acquisition; investigation; methodology; validation; visualization; writing-original draft; writing-review and editing and supervision and project administration.

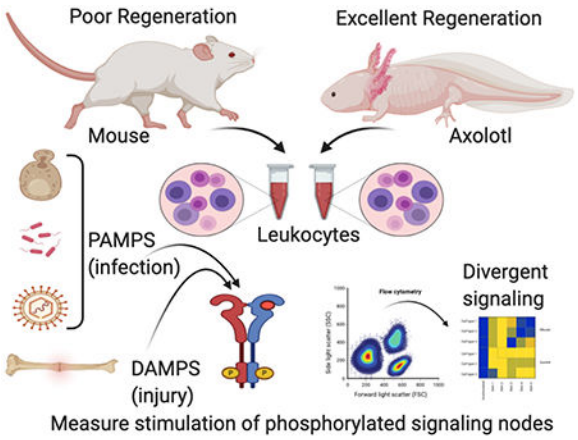

Keywords

Axolotl; salamander; regeneration; macrophages; wound-healing; Toll-like receptor; DAMP; PAMP; inflammation; phospho-flow

1. Introduction

The regulation of inflammation after injury has been proposed as a key factor in determining the quality of wound repair and potential for tissue regeneration. The response to injury in regenerative vertebrates has traditionally been associated with muted or absent pro-inflammatory signaling. The remarkable ability of salamanders to regenerate whole limbs after amputation has been attributed to an immune system prioritized for cellular repair and lacking the advanced adaptive immune responses observed in mammals that confers protection from viruses [1, 2]. Despite this gap in immune protection, salamanders appear to be well equipped to deal with bacterial and fungal threats via innate immune cell surveillance and phagocytosis.

We previously reported a complex inflammatory response after limb amputation in *Ambystoma mexicanum* (Mexican axolotl), a urodele amphibian, that features simultaneous expression of both pro- and anti-inflammatory signaling cascades. Limb regeneration and the inflammatory profile is critically dependent on innate myeloid immune cells (macrophages) without which, regeneration failure and fibrotic scar tissue formation results [3]. Given that limb regrowth takes place in water full of microorganisms it is interesting that the axolotl can achieve tissue regeneration while resisting bacterial or fungal threats that would normally stall or impede healing in mammals. Understanding the molecular basis of regeneration-permissive injury responses in a non-sterile environment may provide important insights for enhancing wound repair in mammals.

In contrast to microbe-triggered inflammation, the molecular signal transduction pathways controlling sterile inflammation in regeneration remain relatively unexplored. Several classes of receptors, collectively termed pattern recognition receptors (PRRs), are important for sensing microorganismal infection and for the subsequent induction of pro-inflammatory responses [4]. Pathogen-associated molecular patterns (PAMPs) are germline encoded PRRs

that sense conserved structural moieties found in microorganisms. It is now evident that PRRs also recognize non-infectious material and endogenous molecules, termed damage-associated molecular patterns (DAMPs). These molecules are sequestered intracellularly under normal physiological conditions, hidden from recognition by the immune system [5]. In cellular stress or injury, DAMPs are released into the extracellular environment by dying cells and trigger sterile inflammation. DAMPs have similar functions as PAMPs in their ability to activate pro-inflammatory pathways and to recruit immune cells to the damaged/infected tissue [5]. Given that injury and infection can occur simultaneously, and that one can lead to the other, it is logical that pathogen- and tissue- mediated damage sensing are linked through common feedback mechanisms to regulate inflammatory stimulation. However, very little is known of the crosstalk between these sensing systems.

The evolutionarily conserved Toll-like-receptor family of pattern receptors allow the sensing of both pathogen (PAMP) and damage (DAMP) molecular pattern molecules [4]. Together they allow transmission of alarm signals associated with injury and infection. Individual TLRs are structurally and functionally distinct but share common motifs such as extracellular leucine-rich repeats (LRR) (required for pathogen recognition) and an intracellular toll/interleukin-1 receptor (TIR) domain (required for the initiation of intracellular signalling) [6]. Specific ligands bind to TLR homodimers or heterodimers with human TLRs 1-9 signalling through myeloid differentiation factor 88 (MyD88) with the exception of endosome-restricted TLR3, which is exclusively via toll-interleukin-1R domain containing adaptor inducing interferon-b (TRIF) [7]. Intracellular signalling is mediated via mitogen-activated protein kinases (MAPKs) such as P38, extracellular signal-regulated kinase (ERK) and c-Jun N-terminal kinase (JNK), as well as interferon regulatory factors (IRFs). These signalling events activate transcription factors such as nuclear factor κB (NF-κB) and AP-1. Ultimately this cascade of signals elicits the cellular release of effector molecules in the form of inflammatory cytokines and other molecules such as nitric oxide (NO) species and reactive oxygen species (ROS) that further regulate the amplification of inflammatory response and the eventual return to homoeostasis (reviewed in [7–9]).

The role of TLRs in pathogen-induced inflammation is well established across most vertebrates. Comparative studies examining TLR-mediated inflammation during tissue injury or the repair process have primarily been conducted in mammals [10–13]. Several studies in mice have implicated TLRs in the repair of various tissues including blood vessels, nerve, skin and bone [14–19]. Given its evolutionary conservation, we hypothesised that the TLR signalling pathway would mediate inflammatory responses in salamanders relevant for regulating myeloid cell phenotypes that are important for regeneration. These studies confirm that invading macrophages are major TLR bearing cell subsets that can respond to both injury and pathogen antigens. We identified several conserved PAMP-dependent signalling responses via TLR-dependent MAPK phosphorylation, using pharmacological inhibition of the MyD88 adaptor protein and quantitation of downstream cytoplasmic NO production and inflammatory gene induction. As TLRs can regulate inflammation in response to injury signals, we took a novel comparative approach examining *in vitro* mammalian and axolotl signal transduction. Testing responses to a cocktail of host derived endogenous ligands revealed an unexpectedly divergent TLR-

mediated signalling response to DAMP ligands that may provide insights on novel responses to injury that underpin the salamander's superior regenerative capacity.

2. Results

2.1 Identification of conserved axolotl TLRs

The TLR repertoire between vertebrate groups ranges from 10-13 in mammals, 21 in teleost fish, with 20 and 21 found in anuran and urodele amphibians respectively [20–22] [23], reviewed in [4]. Many of these TLRs are common to vertebrates containing highly conserved sequence motifs imposed by evolutionary constraints on host defense, whereas others represent species-specific TLRs that possibly reflect fine tuning of responses for divergent host environment pressures.

Specific TLR loci are generally considered to recognize different groups of PAMPs. TLR5 can recognize bacterial flagellin [24]. TLR4 can recognize lipopolysaccharides (LPS) in gram-negative bacteria [25] along with polysaccharide molecules derived from the cell wall/capsule from different fungi species [26]. TLR3 is involved in the recognition of double-stranded RNA (dsRNA) generated as a by-product of viral replication or necrotic cells [27]. TLR2 can recognize PAMPs by cooperating with TLR1 or TLR6 to distinguish between triacyl and diacyl lipopeptides and zymosan, a β-Glucan polysaccharide antigen found in yeast cell walls is recognized by TLR2/TLR6 heterodimer.

In this study we were first interested in confirming the conservation in TLR responses to 3 major microorganismal classes via representative PAMP ligands and their cognate receptors: TLR4 recognizing gram negative bacterial LPS, TLR2 signaling via Zymosan, an antigen found in yeast cell walls, and TLR3 signaling via polyinosinic:polycytidylic acid (Poly I:C) stimulation, a double stranded RNA analog that simulates viral infection. Both TLR2 and TLR3 receptor sequences from salamanders have been previously identified to be present and conserved, however previous attempts to Identify the TLR4 orthologue in salamanders using either the newt or axolotl public transcriptome assemblies were unsuccessful [21]. Using the latest axolotl genome assembly, we were able to isolate the full-length axolotl TLR4 within an expressed region of chromosome 8 and confirmed its identity using synteny analysis and alignment with other vertebrate orthologues (Figure 1). We were also able to confirm the existence of the RP105 protein (CD180) in the axolotl genome, a TLR4 related molecule that shares considerable structural and sequence homology but lacking the C-terminal TIR domain important for recruitment of adaptor proteins required for intracellular TLR signaling [28]. Comparing the TLR2, TLR3, TLR4 and CD180 across humans, mouse, zebrafish, Xenopus and the axolotl we found predictable evolutionary relationships between taxa (i.e., both amphibian genes grouped together and both mammalian genes group together; Fig. 1A).

2.2 *In vivo* PAMP and DAMP induced inflammation recruits TLR enriched myeloid cells

Given the critical role of TLR2, TLR3 and TLR4 signaling in modulating inflammation after PAMP stimulation and sensing tissue damage via DAMPS [5], we set out to compare PAMP stimulation with tissue damage in a limb amputation model.

After limb amputation, TLR2 demonstrated robust upregulation over the time-course of regeneration (Figure 2A). We previously characterized the critical role of innate myeloid immune cells such as monocytes and macrophages in the success of regeneration and the control of inflammation [3]. To investigate the macrophage cellular response to these inflammatory TLR agonists, we employed an established flow cytometry/FACS protocol [29] to identify myeloid and non-myeloid cell populations (Figure 2B). FACS-isolation of blastema cell populations at 4dpa combined with rt-qPCR analysis confirmed a 3.4 and 2.3-fold enrichment of TLR2 and TLR4 transcripts in the IB4+ CD18+ macrophages (Figure 2C). This **suggests** that these myeloid cells are likely to be the primary cells responding to both endogenous and pathogenic TLR ligands in this microenvironment. Measurement of IB4+CD18+ macrophage recruitment via flow cytometry also revealed their robust recruitment to an equivalent position in limb tissue, 48hrs following treatment with either LPS, Zymosa or Poly I:C injections (Figure 2D). This confirms that axolotl macrophages are the likely to be the primary TLR bearing responders to injury or infection.

2.3 Conserved MyD88 dependent MAPK phosphorylation and nitric oxide release in axolotl monocytes following stimulation with pathogen derived TLR agonists

We previously established that macrophage depletion prior to amputation results in failure of limb regeneration and major dysregulation of inflammatory cytokine kinetics [3]. The early salamander cytokine pattern is a mixture of both pro and anti- inflammatory signals and is divergent from mammalian (mouse) tissue injury responses. How myeloid cells drive and regulate the inflammatory response during early limb regeneration is not completely understood. In addition, little is known about how salamanders respond to pathogens present in their surrounding environment during homeostasis and injury. In order to investigate the complex signalling networks leading from TLR engagement to cytokine regulation we began by focussing on AP-1-dependent pro-inflammatory regulation via conserved p38 MAPK and ERK kinase hubs. The intracellular signalling network predicted to be conserved in salamanders is displayed in Figure 3. This serves as a reference pathway for testing TLR signalling with the predicted stimulation of MAPK phosphorylation (via Poly I:C, Zymosan or LPS engagement) highlighted in yellow. Predictions are based on numerous reviews and generalized pathways that are yet to be confirmed by experimental evidence in the axolotl (See [5, 30] for reviews).

As a starting point, we sought to assess whether MAPK phosphorylation following stimulation with TLR ligands was conserved in axolotl peripheral blood mononuclear cells (PBMCs). We first focussed on mapping the immediate intracellular responses to rapid stimulation with PAMP ligands to TLR2-4, a common practice in early mammalian TLR studies. To achieve this, we adapted intracellular phospho-flow cytometry techniques to simultaneously capture phosphorylation of specific epitopes in different cell lineages within the heterogeneous pool of cultured PBMCs without the need for purification procedures [31]. Viable monocytes were selected from the pool of fixed and permeabilised PBMCs during flow cytometry analysis with the aid of cell viability dyes and a cross-reactive anti-human CD18 antibody and axolotl myeloid cell marker IB4 (Figure 4) [29]. The majority of these cells resemble monocytes morphologically, consistent with previous reports [3, 32, 33]. Rapid stimulation of TLR2-4 resulted in detectable increases of both phospho-P38 and

phospho-ERK above baseline median fluorescent intensity (MFI) levels in IB4+ CD18+ but not CD18− PBMCs Figure 4D–H.

In mammals TLR2 and TLR4 both signal through the adaptor molecule MyD88 whereas TLR3 is MyD88 independent. To test whether this signalling pathway was conserved in axolotl PBMCs we next applied the MyD88 pharmacological inhibitor ST2825 prior to TLR stimulation and examined for any prevention in increasing phospho-P38 and ERK MFI levels (n = 8-12 biological replicates per experimental group) [34, 35]. Pre-treatment with ST2825 without TLR stimulation showed non-significant reductions in phospho-P38 and NO MFI levels in IB4+ CD18+ monocytes, and ERK MFI was unaffected (Figure 4H). Consistent with mammalian MyD88 biology, treatment with ST2825 showed reduced phosphorylation of P38 when compared with non-treated TLR stimulated samples, for both LPS-induced TLR4- and zymosan-induced TLR2 signalling. (Figure 4,E,H). ST2825 treatment coupled with Poly I:C stimulation of TLR3 did not result in any reduction of phospho-P38 MFI levels (Figure 4H) indicating the potential conservation of TLR3 signalling via a MyD88 independent pathway. Consistent observations were seen for the phosphorylation of ERK following PAMP-TLR stimulation, notably with zymosan-induced TLR2 causing high MFI levels, which were reduced but not completely inhibited with pre-treatment of ST2825 Figure 4,F, H).

Nitric Oxide (NO) is a key molecule in macrophage phenotype and function [36]. Production of NO during inflammation in mammals is dependent on both MyD88 and MAPKs [37, 38]. Our experiments determined that TLR stimulation of PBMCs resulted in LPS-induced NO-production in both IB4+CD18+ and CD18− populations, with no changes with Zymosan, and only a small non-significant increase in NO production in CD18− cells via Poly I:C stimulation (Figure 4G, H). The addition of either MyD88 (ST2825) or P38 MAPK (SB203850) inhibitors produced significant decreases below baseline in IB4+ CD18+ NO MFI levels (Figure 4G,H). Moreover, inhibition with SB203850 prior to stimulation prevented the return to baseline levels following TLR stimulation with all of the tested agonists. Together these inhibitor studies suggest that the dependency of TLR responses on MyD88 signalling are largely conserved in axolotl.

2.4 Myeloid cells from blastema samples display differential *in vivo* MAPK activity compared with TLR-recruited cells.

Elucidation of signal transduction via phospho-MAPK following tissue injury or infection was again assessed via phospho-flow cytometry Figure 5A. Consistent with our short-term *in vitro* studies, we observed marked increases in phospho-P38 MFI levels in IB4+ CD18+ myeloid cell compartments resulting from long term exposure to PAMP agonists *in vivo*, whilst also revealing remarkable increases in regenerating samples Figure 5B. In contrast, phospho-ERK signalling in both myeloid (IB4+ CD18+ and IB4+ CD18−) and non-myeloid cells (IB4− CD18−) in the limb was globally diminished Figure 5C. IB4+ CD18+ myeloid cells responded similarly to infection and amputation with decreases below baseline NO levels. In contrast, IB4− CD18− cells responded to amputation by increasing NO MFI levels by almost 2-fold but did not change following stimulation with LPS, zymosan or poly I:C Figure 5D

Downstream inflammatory genes were surveyed in limb tissue to further parse out differences in the inflammatory response between injury and delivery of pathogenic TLR ligands. *In vivo* LPS treatment resulted in the activation of known target genes IL-1β (NS), IL-6 ($p<0.05$), TNFa (NS), COX2 ($p<0.0001$) and SOCS3 ($p<0.001$). Zymosan treatment induced IL-1β ($p<0.05$), IL-6 ($p<0.0001$), IL-8 ($p<0.001$), IL-10 ($p<0.05$) and SOCS3 ($p<0.001$) activation. Administration of poly I:C only resulted in signification expression of SOCS3 ($p<0.05$) whilst down-regulating expression of other inflammatory genes such as IL-1β (NS). In comparison, the inflammatory gene signature present in the early blastema displayed the most unique profile and had highest level of induction of most genes tested Figure 5E.

2.5 Axolotls and mice display differential intracellular responses to DAMP agonists *in vitro*.

We next sought to compare the intracellular responses of axolotl and mammalian immune cells to endogenous TLR ligands derived from tissue injury directly. In addition, we investigated how such ligands may regulate PAMP induced TLR signalling. To achieve this, we chose to model the tissue injury response *in vitro* by adapting a recently established technique utilising crushed bone samples that contain a range of endogenous TLR ligands to serve as a surrogate cocktail of DAMPs [39]. Sterile bone crush mixtures (BCM) from donor axolotl and mice limbs were presented to their corresponding PBMCs for 10 minutes. A separate set of BCM treated samples were then subjected to an additional 5-minute stimulation with TLR PAMP ligands. Post-fixation flow cytometry analysis of phospho-P38, phospho-ERK and NO was then performed on axolotl PBMCs using CD18 and IB4 to discriminate monocytes, with mouse monocytes identified with anti-mouse CD11b (Figure 6A). No significant impairments to cell viability occurred in any of the experimental groups thus ruling out any effects relating to cell death Figure 6B. Rapid stimulation of axolotl and mouse monocytes with their donor BCMs resulted in increases in phospho-P38 MFI levels (Figure 6C, G). Consistent with previous reports, BCM treatment results in phosphorylation of P38 in mouse monocytes, but this signal is negatively regulated following application of PAMP agonists [39]. In stark contrast, axolotl samples either maintained or increased phospho-P38 MFI levels after application of PAMP agonists Figure 6C. Further differences were seen upon examining ERK phosphorylation, where BCM stimulation as well as additional application of PAMPs produced modest increases in phospho-ERK MFI levels for axolotl monocytes (except for BCM + LPS) but major decreases in mice (Figure 6D, G). Nitric oxide MFI $\log_2$FC moderately increased in mouse monocytes after BCM stimulation, whereas parallel axolotl samples displayed significant reductions below baseline, and this effect was shown to be independent of source BCM DAMPs through a reciprocal experiment (Figure 6 E, F). Taken together, these differential *in vitro* responses to ligands derived from tissue injury in the presence of pathogen antigens indicate that salamander macrophages may be programmed to respond to differently than mammals within a nonsterile wound environment.

3 Discussion

Initiation of signal cascades in response to pathogen challenge or tissue damage is driven by several innate immune receptor families that synergise to positively or negatively regulate inflammation [40]. To our knowledge, this is the first report describing functional experimentation of the TLR signalling pathway in urodele amphibians, a model most commonly studied for their unique regenerative properties. Previous studies have illustrated the importance of inflammatory regulation during tissue regeneration in amphibians via administration of immune-modulating agents [41, 42]. We further explore this theme by introducing pathogen-associated and damage-associate ligands, to induce inflammation and assess for conserved signalling responses. To this end, we have adapted phospho-flow cytometry to measure rapid intracellular signalling changes, as it affords the ability to utilise minimal tissue without the necessity for pooling samples. Further, the added ability to monitor single cell changes within a specific cell lineage, as identified by extracellular markers, renders purification steps obsolete and allows rapid profiling of heterogeneous cell sources [31]. These techniques can be applied to a range of other phosphorylation-dependent signalling pathways to obtain cell-type-specific signalling information, not accessible using traditional ratio-metric western blotting tools.

During inflammation, MAPKs act as a signalling node in between ligand binding and activation of gene expression in the nucleus [43]. Our *in vitro* and *in vivo* experiments reveal that TLR stimulation results in an evolutionarily conserved activation of this signalling pathway. Further investigation found that zymosan-induced TLR2 signalling and LPS induced TLR4 signalling are dependent on the presence of MyD88, consistent with mammalian TLR biology [7]. Conserved throughout evolution, MyD88 acts as the main adaptor for the majority of TLR recognition signal transduction [43, 44]. Though its role in tissue regeneration has yet to be explored thoroughly, recent evidence from the mouse suggests MyD88 may negatively impact regeneration at least in the context of mesenchymal-stem-cell driven bone repair [19]. Our study identified nitric oxide (NO) as a conserved downstream target of monocyte TLR-MyD88- P38-MAPK signalling *in vitro*, suggesting that it may play a potential role as a potent pro-inflammatory molecule. *In vivo*, iNOS$^{-/-}$ mice display defective muscle regeneration capabilities, and during injury nitric oxide expression is restricted to macrophages following skeletal muscle damage [45]. In contrast to mouse macrophages, we found that that axolotl IB4+ CD18+ macrophages gradually reduce NO levels upon injury. During this period, non-myeloid cells concurrently increase intracellular NO levels suggesting that non-immune cells resident in the limb can release pro-inflammatory signals. This fits with separate observations where reactive oxygen species (ROS) are activated early in injury to recruit immune cells. ROS signalling not only plays a role as an anti-microbial but can also alter developmental pathways important for tadpole regeneration [46].

Consistent with our previous report [3], early limb regeneration displays a unique inflammatory signature with a high level of induction in both pro-inflammatory and anti-inflammatory genes (Figure 5). This is striking when considering *in vivo* application of pathogenic TLR agonists did not induce comparable amplitude increases for most genes examined. Overall, out of all the TLRs tested, TLR3 was consistently the weakest driver

of inflammatory responses both in our in vitro PBMC cultures and the limb *in vivo* model. In mammals, TLR3 has been noted for its importance in mediating inflammation after skin injury that can be modulated by cutaneous microflora [47, 48]. Poly I:C-induced TLR3 signalling displayed minor MAPK activation and the weakest inflammatory response, both short-term *in vitro* and long term *in vivo*. Our findings further add to the weight of evidence regarding the salamanders attenuated adaptive immune system. The lack of robust TLR3 responsiveness supports previous reports of poor viral immunity [49]. Of great interest is determining how axolotl TLR3 signals to the nucleus following pathogen recognition. Our results show that LPS does induce MAPK driven inflammation. This is in line with several studies reporting robust biological responses in axolotls following LPS stimulation [3, 50] and this study confirms the existence of Axolotl TLR4 and the related CD180 molecule. CD180 has the potential for crosstalk with TLR4 and competes for ligand binding [51]. Further studies are required to examine TLR regulation in salamanders and provide greater evolutionary insights on the lack of TLR4-mediated LPS sensitivity in some fish species. [52, 53]. TLR2 is the most dramatically regulated TLR in the regenerating limb and this receptor is predominantly in IB4+ CD18+ macrophages. Conserved TLR2 responsiveness is not surprising given that TLR2 is present in almost all vertebrates and functions to recognise a wide range of lipoproteins present in multiple pathogens [54], The specific role of TLR2 in limb regeneration remains to be explored.

Our study primarily focused on mapping TLR responses to a broad range of DAMPs *in vitro* with the BCM model, and *in vivo* with limb amputation. Several other studies have implicated roles for DAMPs in tissue repair signalling through TLRs. Strong evidence from ischemia/reperfusion injury models of the mammalian heart, lung and liver have provided several endogenous TLR2 and TLR4 ligand candidates that regulate tissue repair such as HMGB1, heat shock proteins (HSPs) and hyaluronan [11, 12, 55–58]. In zebrafish, HMGB1 has been implicated in spinal cord regeneration and hsp60 is essential for fin blastema formation and outgrowth [59, 60]. Interestingly hsp60 has been shown to bind with LPS to synergise TLR4-induced innate and adaptive immune responses [61]. Our *in vitro* experiments examining the axolotl response to injury signals and subsequent TLR pathogen challenge also suggests TLR synergy in this setting, however the mechanism remains unknown. On the other hand, signalling responses in mice directly oppose those of axolotl and prioritised negative regulation of TLR-MAPK signalling. Several possibilities could account for this disparity. An intriguing speculation is that the mammalian inflammatory response may be biased towards efficiently clearing pathogens by exacerbating pro-inflammatory signals and cell death. However, this may come at the expense of fibrosis-free wound repair such as occurs in salamanders, which ably tolerate non-viral pathogens and develop balanced inflammatory micro-environments following injury.

4 Conclusions:

The deficiency in molecular information regarding inflammatory signalling in regenerative organisms is a barrier to improving the transition between wound healing and regeneration in mammals. To fill this gap in knowledge, we have provided the first evidence for conserved TLR-MAPK signalling in the axolotl. Importantly, we show that myeloid cells

are the primary contributors to TLR signalling in peripheral blood and the limb and may aid in the recruitment of additional leukocytes to the site of inflammation. The phospho-flow approach couples flow cytometry with cell signalling analysis, on a single cell and population level. This allowed us to identify conserved myD88 dependent-MAPK signalling with PAMP agonist activation in both axolotl macrophage and non-macrophage cell types. In comparative studies between macrophages from the mouse or axolotl, partial conservation of p38-MAPK within macrophages in response to stimulation with endogenous DAMP ligands was observed but divergent responses in ERK and downstream NO signalling. Of particular note, the effects of DAMP stimulation prior to PAMP stimulation revealed alternative programming in response to a mixed (DAMP/PAMP) damage/pathogen signalling environment. These differences in signalling may indicate an innate response in axolotl macrophages that primes them for a response to non-sterile injury that favours regeneration over scar tissue formation.

This study focussed on MAPK-dependent signalling hub upstream of AP1 transcription factor- dependent pro-inflammatory cytokines. With additional tool development, future work will be aimed at examining the role the NF-κB transcription factor, another major regulator of pro-inflammatory cytokine expression in vertebrates. Regulation of Type I interferon through TLR3 which was also not addressed. Despite these limitations, this work opens the door for further mapping and identification of critical nodes in TLR signalling pathways that may regulate the unique inflammatory environment permissive for axolotl limb regeneration and scar free repair in the presence of microorganisms.

5 Experimental Procedures

5.1 Animal strains and husbandry

All animal care protocols and methods were performed in accordance with relevant regulations and guidelines and with approval from either the Monash University animal ethics committee (AEC), The Jackson Laboratory or MDIBL (IACUC) animal care and use committees. *Ambystoma* mexicanum (Mexican axolotl) were individually housed in carbon-filtered tap water or 20% Holtfreter's solution on a 12-hour light, 12-hour dark cycle. Adult axolotls were used for all experiments and were at least 12-months old measuring between 15-20 cm (snout to tail). Prior to blood collection, amputation or in vivo stimulation, animals were anaesthetized using 0.1% ethyl-3-aminobenzoate methanesulfonate salt (MS-222; Sigma-Aldrich).

Adult 10–16-week-old C57BL6/J Mus *Musculus* (mice) were used as the reference strain for the collection of leukocytes in *ex vivo* comparative TLR activation experiments.

5.2 TLR sequence analysis

Human, mouse, zebrafish and xenopus TLR translated nucleated sequences were obtained from the National Centre for Biotechnology Information (NCBI). Axolotl TLR translated nucleated sequences were obtained from https://www.axolotl-omics.org/ using Assembly Am_3.4 and Genome Assembly v6.0-DD.

To identify the missing TLR4 sequence, we first BLASTed the human TLR4 protein against the axolotl transcriptome assembly [62] and found a fragmented transcript that corresponded to a single exon of the Tlr4 gene. Next, we aligned that transcript to the axolotl genome assembly with RNA expression tracks loaded. Since the transcript only represented a fragment of the gene, we looked at the genes both upstream and downstream of that fragment to use the synteny to confirm that the genomic region (green) was correct. We then only focused on the region between two closest neighboring genes BRINP1 (orange) and ASTN2 (yellow) and used synteny to identify the full TLR4 sequence and exons. Axolotl TLR4 cDNA was given the GenBank accession number MW506838. Multiple sequence alignments were performed with MAFFT using L-INS-I strategy and the BLOSUM62 substitution matrix. Axolotl-Human protein sequence alignments were displayed using Jalview [63]. Phylogenetic trees were constructed with the neighbour-joining method with 1,000 bootstrap replicates from a matrix of JTT distances in MEGA7 and using model-based Bayesian inference in MrBayes 3.2.2 [64, 65]. Bayesian analysis was run for $1x10^6$ steps with trees sampled every 200 steps and the first 25% of sampled trees discarded. Predicted axolotl TLR2 and TLR3 and human TLR2 and TLR3 protein domains were generated using SMART (Simple Modular Architecture Research Tool) web resource tool (http://smart.embl.de).

5.3 Isolation and stimulation of primary axolotl peripheral blood mononuclear cells

Axolotl peripheral blood was isolated as previously described [29]. Briefly, peripheral blood was collected using a 25G SURFLO® winged infusion set (Terumo Medical Products) into 50 mL tubes containing ice cold 0.7X HBSS-5 mM EDTA. Cells were then centrifuged at 350 x g to remove clots. Peripheral blood mononuclear cells (PBMCs) were enriched for using Ficoll-Paque Plus (GE Healthcare Life Sciences). Centrifugation was adjusted to 8 minutes at 400 x g to obtain PBMCs within the buffy coat. Isolated PBMCs were incubated in 0.7X HBSS-2% goat serum-5 mM EDTA on ice or at 4°C. Collected peripheral mouse blood underwent same post collection processing with the following alterations: use if 1X HBSS-5 mM EDTA and a 40-minute duration for the centrifugation stage of PBMC isolation with Ficoll-Paque Plus. TLR stimulation was performed using the following PAMP agonists: LPS (1 μg/mL), Zymosan A (200 μg/mL) and Poly I:C (100 μg/mL) for 10 minutes of stimulation before washing. Bone Crush Mixture (BCM, a DAMP agonist, was used at 200 μg/mL) for 10 minutes of stimulation before washing or if used in combination with PAMP agonists, BCM was pre-incubated for 5 minutes before addition of the PAMP agonist, incubated a further 10 minutes then washed. BCM agonist was prepared using femurs from euthanized donor mice or axolotls extracted under sterile conditions. 40mg of bone tissue was crushed using a sterile mortar and snap frozen in liquid nitrogen. This homogenized tissue was resuspended in 400μl of sterile HBSS to make a 100mg/mL stock. The BCM was subjected to 2 rounds of freeze-thaw at −80°C/RT before use as an agonist. SB202190 (20 μM) (Calbiochem) and ST2825 (50 μM) (MedChem Express) were used over 12-hour incubation time periods to inhibit P38 and MyD88 respectively.

5.4 In vivo limb stimulation with TLR agonists and limb amputation

Right forelimbs of anaesthetized axolotls were injected sub-dermally with LPS (1 μg/mL), Zymosan A (200 μg/mL) and Poly I:C (100 μg/mL). Sterile saline solution was used for all

control injections. Limb tissue was collected 48 hours post injection and either harvested for RNA or flow cytometry analysis. Limb amputation and tissue collection/processing for flow cytometry analysis were performed as previously described [29].

5.5 cDNA synthesis and RT-qPCR

Both cell suspensions and limb tissues samples were collected into TRIzol® reagents (Thermo Fisher Scientific. RNA was purified using Direct-zol™ RNA MiniPrep (Zymo Research) according to manufacturer's instructions. RNA quality was assessed by spectrophotometry using a NanoDrop ND-1000 (NanoDrop). Reverse transcription was performed using SuperScript® VILO™ cDNA synthesis kit (Thermo Fisher Scientific). Quantitative Polymerase Chain Reaction (qPCR) assays were performed using LightCycler® 480 SYBR green (Roche). Gene expression levels were calculated using the $2^{-\Delta\Delta Ct}$ method. Sample gene expression was normalised to the geometric mean of 3 housekeeping genes and either expressed as relative fold change or $\log_2$ fold change. Primer sequences used in qPCR assays are listed in Methods Table 1.

5.6 Flow cytometry and FACS

Cell viability was assessed with Ghost Dye™ Red 780 (Tonbo Biosciences) and was added to cell suspension per manufacturer's instructions prior to intracellular staining. Intracellular nitric oxide levels were assessed by incubating 5 μM DAF-FM DA to single cell suspensions for 30 minutes on ice following incubations with TLR agonists and or p38/MyD88 inhibitors. After incubation, cells were washed with 0.7X HBSS-2% goat serum-5 mM EDTA and centrifuged for 10 minutes at 350 x g to allow complete de-esterification of the intracellular diacetates. Cells were fixed with 1.5% PFA for 15 minutes at room temperature and wash with 0.7X HBSS. Cells were then permeabilized with 100% ice-cold methanol for 10 minutes at 4°C after which cells were then stored at −20°C overnight. Blocking was performed with 0.7X HBSS-2%-goat serum 5 mM EDTA for 20 minutes on ice after which a mixture of primary antibodies was then added and incubated for 1 hour on ice. Primary antibodies were washed, and cells were then incubated with their corresponding secondary antibody for 30 minutes on ice. Cells were then washed transferred into FACS tubes for flow cytometry analysis. Flow cytometry experiments were conducted on LSR II Fortessa Flow Cytometers (BD Biosciences) or LSR II Flow Cytometers (BD Biosciences). Compensation of fluorescence spectral overlap was used with UltraComp eBeads (eBioscience) according to manufacturer's instructions. FCS 3.0 files generated by flow cytometry were analysed using FlowJo Software (Tree Star). Live cells isolated via FACS received the same blocking and staining protocol but did not undergo fixation or permeabilization. Viable cells isolated during FACS were identified with aid of DAPI. All cells were sorted using BD Influx Cell Sorter (BD Biosciences). Details of antibodies used are in Methods Table 2.

5.7 Modified Giemsa-Wright Stain

Staining was performed as described in [29]. Briefly, FACS isolated cells were transferred onto poly-L-lysine slides via a Cytospin centrifuge after which cells were fixed in 4% PFA. Cells were stained working dilution May-Grunwald staining solution for 5 minutes and

Giemsa staining solution for 15 minutes with brief washes in distilled water between steps. Slides were then air-dried preserved in DEPEX and imaged under a light microscope.

5.8 Statistical Analysis

Heatmaps and Statistical analyses were performed using Prism 8 (GraphPad Software). Data are always shown as mean values ± SEM. Analyses of significant differences between means were performed using one-way ANOVA or unpaired Student's t-test as indicated.

Acknowledgements

Research reported in this publication was supported by an Institutional Development Award (IDeA) from the National Institute of General Medical Sciences of the National Institutes of Health under grant numbers P20GM103423 and P20GM104318 to MDI Biological Laboratory. The Australian Regenerative Medicine Institute (ARMI) is supported by grants from the State Government of Victoria and the Australian Government. Mouse studies were supported by Jackson Laboratory (JAX) institutional funds. We thank Jim Coffman for careful reading of the manuscript.

REFERENCES

1. Godwin JW and Rosenthal N, Scar-free wound healing and regeneration in amphibians: immunological influences on regenerative success. Differentiation; research in biological diversity, 2014. 87(1-2): p. 66–75. [PubMed: 24565918]
2. Mescher AL, Neff AW, and King MW, Inflammation and immunity in organ regeneration. Developmental & Comparative Immunology, 2017. 66: p. 98–110. [PubMed: 26891614]
3. Godwin JW, Pinto AR, and Rosenthal NA, Macrophages are required for adult salamander limb regeneration. Proceedings of the National Academy of Sciences of the United States of America, 2013. 110(23): p. 9415–9420. [PubMed: 23690624]
4. Nie L, et al. , Toll-Like Receptors, Associated Biological Roles, and Signaling Networks in Non-Mammals. Frontiers in Immunology, 2018. 9.
5. Gong T, et al. , DAMP-sensing receptors in sterile inflammation and inflammatory diseases. Nature Reviews Immunology, 2020. 20(2): p. 95–112.
6. Mikami T, et al. , Molecular evolution of vertebrate Toll-like receptors: evolutionary rate difference between their leucine-rich repeats and their TIR domains. Gene, 2012. 503(2): p. 235–43. [PubMed: 22587897]
7. Kawai T and Akira S, Toll-like receptors and their crosstalk with other innate receptors in infection and immunity. Immunity, 2011. 34(5): p. 637–50. [PubMed: 21616434]
8. Huebener P and Schwabe RF, Regulation of wound healing and organ fibrosis by toll-like receptors. Biochimica et biophysica acta, 2013. 1832(7): p. 1005–1017. [PubMed: 23220258]
9. Barton GM and Kagan JC, A cell biological view of Toll-like receptor function: regulation through compartmentalization. Nat Rev Immunol, 2009. 9(8): p. 535–42. [PubMed: 19556980]
10. Oyama J, et al. , Reduced myocardial ischemia-reperfusion injury in toll-like receptor 4-deficient mice. Circulation, 2004. 109(6): p. 784–9. [PubMed: 14970116]
11. Tsung A, et al. , The nuclear factor HMGB1 mediates hepatic injury after murine liver ischemia-reperfusion. J Exp Med, 2005. 201(7): p. 1135–43. [PubMed: 15795240]
12. Wu H, et al. , TLR4 activation mediates kidney ischemia/reperfusion injury. J Clin Invest, 2007. 117(10): p. 2847–59. [PubMed: 17853945]
13. Tang SC, et al. , Pivotal role for neuronal Toll-like receptors in ischemic brain injury and functional deficits. Proc Natl Acad Sci U S A, 2007. 104(34): p. 13798–803. [PubMed: 17693552]
14. Pinhal-Enfield G, et al. , An Angiogenic Switch in Macrophages Involving Synergy between Toll-Like Receptors 2, 4, 7, and 9 and Adenosine A2A Receptors. The American Journal of Pathology, 2003. 163(2): p. 711–721. [PubMed: 12875990]
15. Aplin AC, et al. , Regulation of angiogenesis, mural cell recruitment and adventitial macrophage behavior by Toll-like receptors. Angiogenesis, 2014. 17(1): p. 147–61. [PubMed: 24091496]

16. Grote K, et al. , Toll-like receptor 2/6 stimulation promotes angiogenesis via GM-CSF as a potential strategy for immune defense and tissue regeneration. Blood, 2010. 115(12): p. 2543–52. [PubMed: 20056792]
17. Wu SC, et al. , Knockout of TLR4 and TLR2 impair the nerve regeneration by delayed demyelination but not remyelination. J Biomed Sci, 2013. 20: p. 62. [PubMed: 23984978]
18. Suga H, et al. , TLR4, rather than TLR2, regulates wound healing through TGF-beta and CCL5 expression. J Dermatol Sci, 2014. 73(2): p. 117–24. [PubMed: 24252748]
19. Martino MM, et al. , Inhibition of IL-1R1/MyD88 signalling promotes mesenchymal stem cell-driven tissue regeneration. Nat Commun, 2016. 7: p. 11051. [PubMed: 27001940]
20. Takeda K, Kaisho T, and Akira S, Toll-Like Receptors. Annual Review of Immunology, 2003. 21(1): p. 335–376.
21. Babik W, et al. , Constraint and Adaptation in newt Toll-Like Receptor Genes. Genome Biology and Evolution, 2015. 7(1): p. 81–95.
22. Kanwal Z, et al. , Comparative studies of Toll-like receptor signalling using zebrafish. Dev Comp Immunol, 2014. 46(1): p. 35–52. [PubMed: 24560981]
23. Ishii A, et al. , Phylogenetic and expression analysis of amphibian Xenopus Toll-like receptors. Immunogenetics, 2007. 59(4): p. 281–93. [PubMed: 17265063]
24. Voogdt CGP, et al. , Reptile Toll-like receptor 5 unveils adaptive evolution of bacterial flagellin recognition. Scientific Reports, 2016. 6(1): p. 19046. [PubMed: 26738735]
25. Poltorak A, Defective LPS Signaling in C3H/HeJ and C57BL/10ScCr Mice: Mutations in Tlr4 Gene. Science, 1998. 282(5396): p. 2085–2088. [PubMed: 9851930]
26. Roeder A, et al. , Toll-like receptors as key mediators in innate antifungal immunity. Medical Mycology, 2004. 42(6): p. 485–498. [PubMed: 15682636]
27. Chattopadhyay S and Sen GC, dsRNA-Activation of TLR3 and RLR Signaling: Gene Induction-Dependent and Independent Effects. Journal of Interferon & Cytokine Research, 2014. 34(6): p. 427–436. [PubMed: 24905199]
28. O'Neill LAJ and Bowie AG, The family of five: TIR-domain-containing adaptors in Toll-like receptor signalling. Nature Reviews Immunology, 2007. 7(5): p. 353–364.
29. Debuque RJ and Godwin JW, Methods for axolotl blood collection, intravenous injection, and efficient leukocyte isolation from peripheral blood and the regenerating limb. Methods in molecular biology (Clifton, N.J.), 2015. 1290 (Chapter 17): p. 205–226.
30. Anwar MA, Basith S, and Choi S, Negative regulatory approaches to the attenuation of Toll-like receptor signaling. Experimental & Molecular Medicine, 2013. 45(2): p. e11–e11. [PubMed: 23429360]
31. Krutzik PO, et al. , Phospho flow cytometry methods for the analysis of kinase signaling in cell lines and primary human blood samples. Methods Mol Biol, 2011. 699: p. 179–202. [PubMed: 21116984]
32. Lopez D, et al. , Mapping hematopoiesis in a fully regenerative vertebrate: the axolotl. Blood, 2014. 124(8): p. 1232–1241. [PubMed: 24802774]
33. Seifert AW, et al. , Skin Regeneration in Adult Axolotls: A Blueprint for Scar-Free Healing in Vertebrates. PloS one, 2012. 7(4): p. e32875. [PubMed: 22485136]
34. Loiarro M, et al. , Pivotal Advance: Inhibition of MyD88 dimerization and recruitment of IRAK1 and IRAK4 by a novel peptidomimetic compound. J Leukoc Biol, 2007. 82(4): p. 801–10. [PubMed: 17548806]
35. Bagchi A, et al. , MyD88-dependent and MyD88-independent pathways in synergy, priming, and tolerance between TLR agonists. J Immunol, 2007. 178(2): p. 1164–71. [PubMed: 17202381]
36. Xue Q, et al. , Regulation of iNOS on Immune Cells and Its Role in Diseases. International Journal of Molecular Sciences, 2018. 19(12): p. 3805.
37. Bogdan C, Nitric oxide and the immune response. Nat Immunol, 2001. 2(10): p. 907–16. [PubMed: 11577346]
38. Mizel SB, et al. , Induction of macrophage nitric oxide production by Gram-negative flagellin involves signaling via heteromeric Toll-like receptor 5/Toll-like receptor 4 complexes. J Immunol, 2003. 170(12): p. 6217–23. [PubMed: 12794153]

39. Li Z, et al. , Tissue damage negatively regulates LPS-induced macrophage necroptosis. Cell Death Differ, 2016. 23(9): p. 1428–47. [PubMed: 26943325]
40. O'Neill LAJ, When Signaling Pathways Collide: Positive and Negative Regulation of Toll-like Receptor Signal Transduction. Immunity, 2008. 29(1): p. 12–20. [PubMed: 18631453]
41. Schotté OE and Sicard RE, Cyclophosphamide-induced leukopenia and suppression of limb regeneration in the adult newt, notophthalmus viridescens. The Journal of experimental zoology, 1982. 222(2): p. 199–202. [PubMed: 7130931]
42. Mescher AL, Neff AW, and King MW, Changes in the Inflammatory Response to Injury and Its Resolution during the Loss of Regenerative Capacity in Developing Xenopus Limbs. PloS one, 2013. 8(11): p. e80477. [PubMed: 24278286]
43. Dong C, Davis RJ, and Flavell RA, MAP kinases in the immune response. Annu Rev Immunol, 2002. 20: p. 55–72. [PubMed: 11861597]
44. Rodet F, et al. , Hm-MyD88 and Hm-SARM: two key regulators of the neuroimmune system and neural repair in the medicinal leech. Sci Rep, 2015. 5: p. 9624. [PubMed: 25880897]
45. Rigamonti E, et al. , Requirement of inducible nitric oxide synthase for skeletal muscle regeneration after acute damage. J Immunol, 2013. 190(4): p. 1767–77. [PubMed: 23335752]
46. Love NR, et al. , Amputation-induced reactive oxygen species are required for successful Xenopus tadpole tail regeneration. Nat. Cell Biology 2013: 15(2)p. 222–228. [PubMed: 23314862]
47. Lin Q, et al. , Toll-like receptor 3 ligand polyinosinic:polycytidylic acid promotes wound healing in human and murine skin. J Invest Dermatol, 2012. 132(8): p. 2085–92. [PubMed: 22572822]
48. Lai Y, et al. , Commensal bacteria regulate Toll-like receptor 3-dependent inflammation after skin injury. Nat Med, 2009. 15(12): p. 1377–82. [PubMed: 19966777]
49. Cotter JD, et al. , Transcriptional response of Mexican axolotls to Ambystoma tigrinum virus (ATV) infection. BMC Genomics, 2008. 9(1): p. 493. [PubMed: 18937860]
50. Salvadori F and Tournefier A, Activation by mitogens and superantigens of axolotl lymphocytes: functional characterization and ontogenic study. Immunology, 1996. 88(4): p. 586–592. [PubMed: 8881761]
51. Divanovic S, et al. , Negative regulation of Toll-like receptor 4 signaling by the Toll-like receptor homolog RP105. Nature Immunology, 2005. 6(6): p. 571–578. [PubMed: 15852007]
52. Iliev DB, et al. , Endotoxin recognition: in fish or not in fish? FEBS Lett, 2005. 579(29): p. 6519–28. [PubMed: 16297386]
53. Sepulcre MP, et al. , Evolution of lipopolysaccharide (LPS) recognition and signaling: fish TLR4 does not recognize LPS and negatively regulates NF-kappaB activation. J Immunol, 2009. 182(4): p. 1836–45. [PubMed: 19201835]
54. Roach JC, et al. , The evolution of vertebrate Toll-like receptors. Proc Natl Acad Sci U S A, 2005. 102(27): p. 9577–82. [PubMed: 15976025]
55. Dybdahl B, et al. , Inflammatory response after open heart surgery: release of heat-shock protein 70 and signaling through toll-like receptor-4. Circulation, 2002. 105(6): p. 685–90. [PubMed: 11839622]
56. Asea A, et al. , Novel signal transduction pathway utilized by extracellular HSP70: role of toll-like receptor (TLR) 2 and TLR4. J Biol Chem, 2002. 277(17): p. 15028–34. [PubMed: 11836257]
57. Jiang D, et al. , Regulation of lung injury and repair by Toll-like receptors and hyaluronan. Nat Med, 2005. 11(11): p. 1173–9. [PubMed: 16244651]
58. Scheibner KA, et al. , Hyaluronan fragments act as an endogenous danger signal by engaging TLR2. J Immunol, 2006. 177(2): p. 1272–81. [PubMed: 16818787]
59. Fang P, et al. , HMGB1 contributes to regeneration after spinal cord injury in adult zebrafish. Mol Neurobiol, 2014. 49(1): p. 472–83. [PubMed: 23996344]
60. Makino S, et al. , Heat-shock protein 60 is required for blastema formation and maintenance during regeneration. Proc Natl Acad Sci U S A, 2005. 102(41): p. 14599–604. [PubMed: 16204379]
61. Osterloh A, et al. , Synergistic and differential modulation of immune responses by Hsp60 and lipopolysaccharide. J Biol Chem, 2007. 282(7): p. 4669–80. [PubMed: 17164250]

62. Nowoshilow S and Tanaka EM, Introducing www.axolotl-omics.org - an integrated - omics data portal for the axolotl research community. Exp Cell Res, 2020. 394(1): p. 112143. [PubMed: 32540400]

63. Waterhouse AM, et al. , Jalview Version 2--a multiple sequence alignment editor and analysis workbench. Bioinformatics, 2009. 25(9): p. 1189–91. [PubMed: 19151095]

64. Kumar S, Stecher G, and Tamura K, MEGA7: Molecular Evolutionary Genetics Analysis Version 7.0 for Bigger Datasets. Mol Biol Evol, 2016. 33(7): p. 1870–4. [PubMed: 27004904]

65. Ronquist F and Huelsenbeck JP, MrBayes 3: Bayesian phylogenetic inference under mixed models. Bioinformatics, 2003. 19(12): p. 1572–4. [PubMed: 12912839]

Key Findings:

- Missing salamander TLR4 gene identified and shows high structural motif conservation with other species.
- New phospho-flow tools developed to measure downstream signaling in multiple salamander cell types.
- Macrophages are a major TLR bearing cell type recruited to the regenerating limb.
- Signaling responses to PAMP agonists are largely conserved between salamander and mouse leukocytes.
- Macrophage responses to PAMPS in the presence of damage antigens are divergent between salamanders and mice.

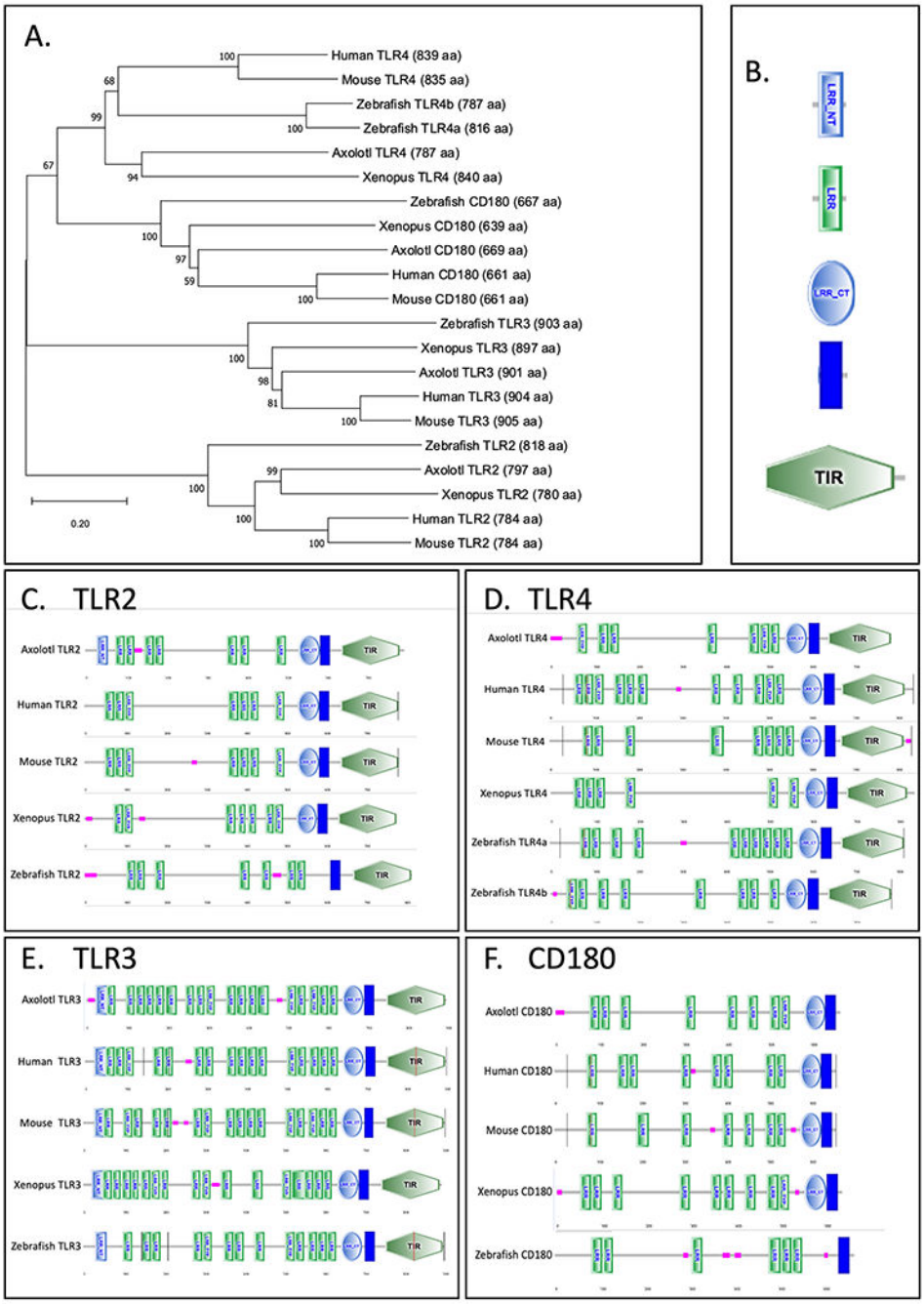

Figure 1. Sequence conservation of axolotl TLRs.

(A) Representative phylogenetic tree of orthologous TLR2-4 generated by MEGA X. Scale bar indicates the evolutionary distance of 0.2 amino acid substitutions per site in the TLRs. **(B)** Abbreviations of annotations: LRR-NT = leucine-rich repeat N-terminal. LRR = leucine-rich repeat. LRR-CT = leucine-rich repeat C-terminal. LRR-TYP = leucine-rich repeat typical. TIR = toll/interleukin-1 receptor homology domain. Pink rectangle indicates low-complexity region. Blue rectangle represents the transmembrane domain.

(C-F) Comparison of the SMART predicted domain structure of axolotl TLR2-4 to other vertebrate species.

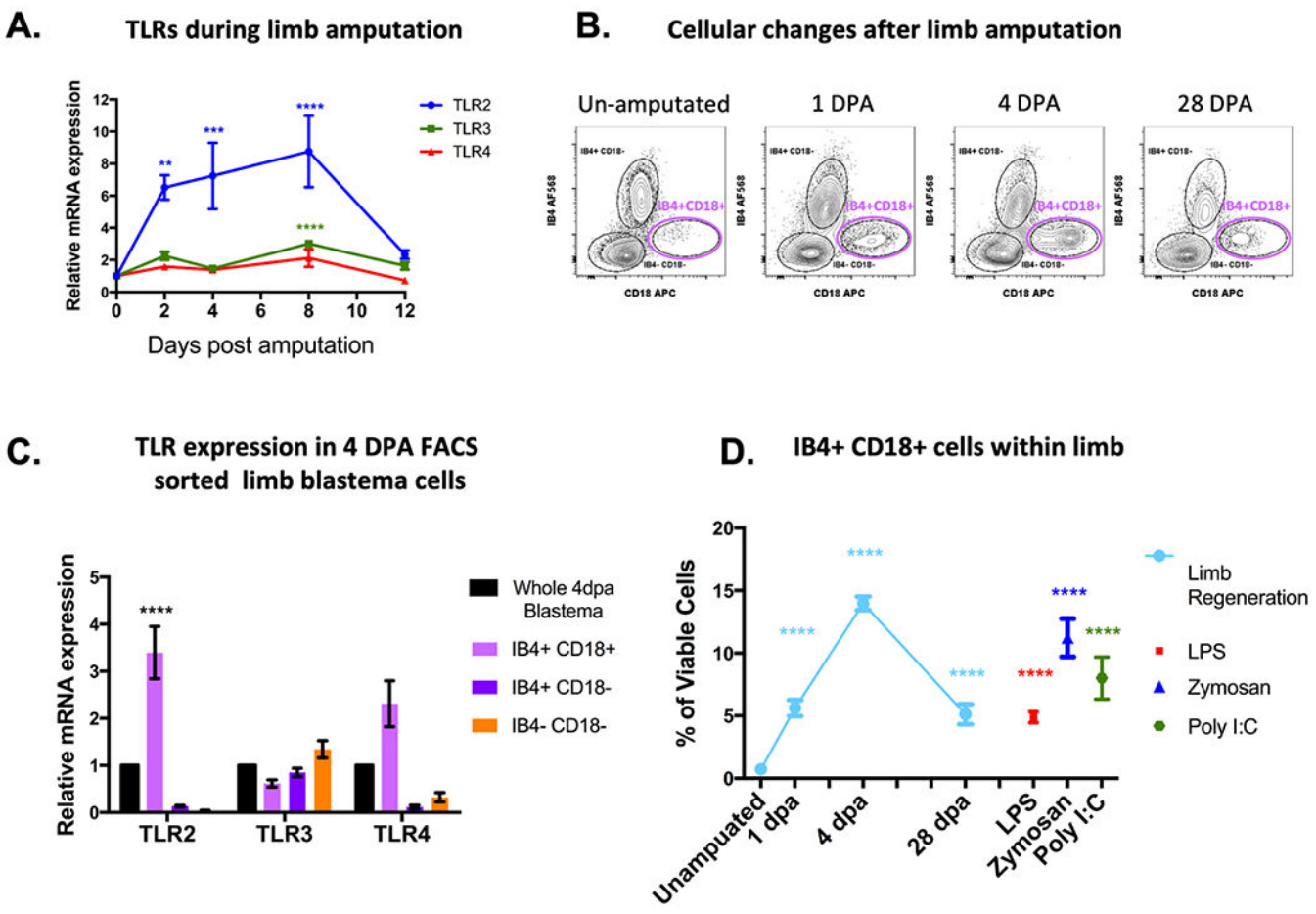

Figure 2. Macrophages are the major TLR bearing subset attending limb regeneration and are responsive to TLR ligands *in vivo.*

(A) Changes in TLR mRNA expression measured by quantitative RT-PCR. Connected line graphs represent ± SEM of 4 biological samples. Adjusted p-values are relative to TLR expression in un-amputated sampled and were obtained via 2-way ANOVA Dunnet's test with multiple comparisons to the un-amputated sample. **P ≤ 0.01, *** P ≤ 0.001 **** P ≤ 0.0001. **(B)** Representative flow cytometry plots of myeloid and non-myeloid cell populations within limb blastema tissue. IB4+CD18+ macrophages highlighted in magenta. (**C)** TLR mRNA expression in FACS isolated limb blastema populations. Bar charts show ± SEM of 3 biological samples**). (D)** Flow cytometry quantification of IB4+ CD18+ cells during several stages of limb regeneration compared with recruitment via *in vivo* TLR stimulation. Plots show ± SEM of 5 biological sample. Adjusted p-values obtained via 2-way ANOVA Dunnet's test with multiple comparisons to the un-amputated sample. **** P ≤ 0.0001.

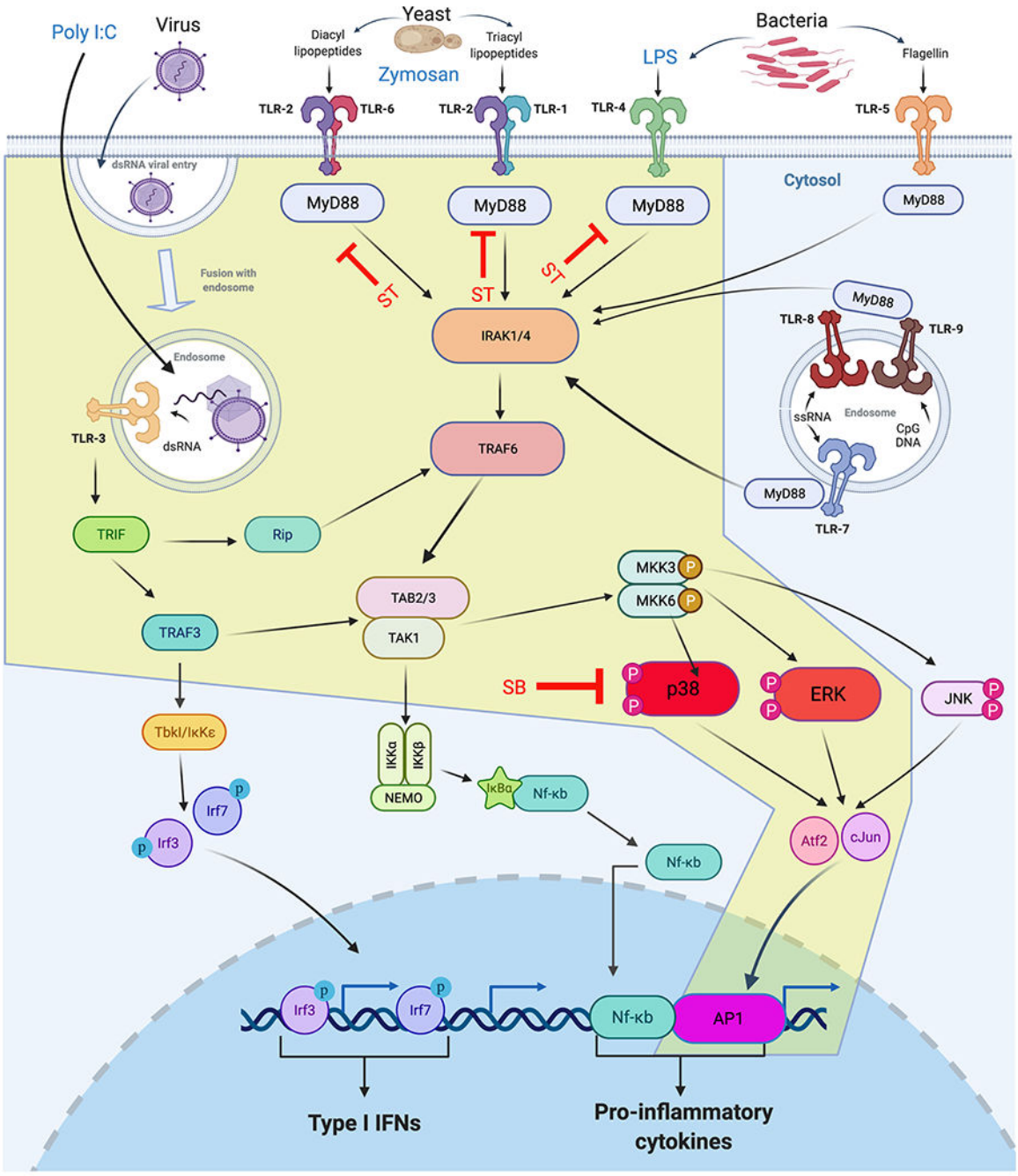

Figure 3.

The predicted intracellular TLR signalling reference network to be tested in salamanders. Antigens from Bacteria, yeast or virally infected cells are predicted to activate specific TLR dimeric receptors that signal through several distinct pathways converging on pro-inflammatory or Type I interferon cytokine responses. The API transcription factor-dependent pathway predicted to signal through p38-MAPK and p-ERK (tested in this study) is highlighted in yellow. Small molecule inhibitors used are shown in red: ST= MyD88 pharmacological inhibitor ST2825. SB= P38 MAPK (SB203850) inhibitor.

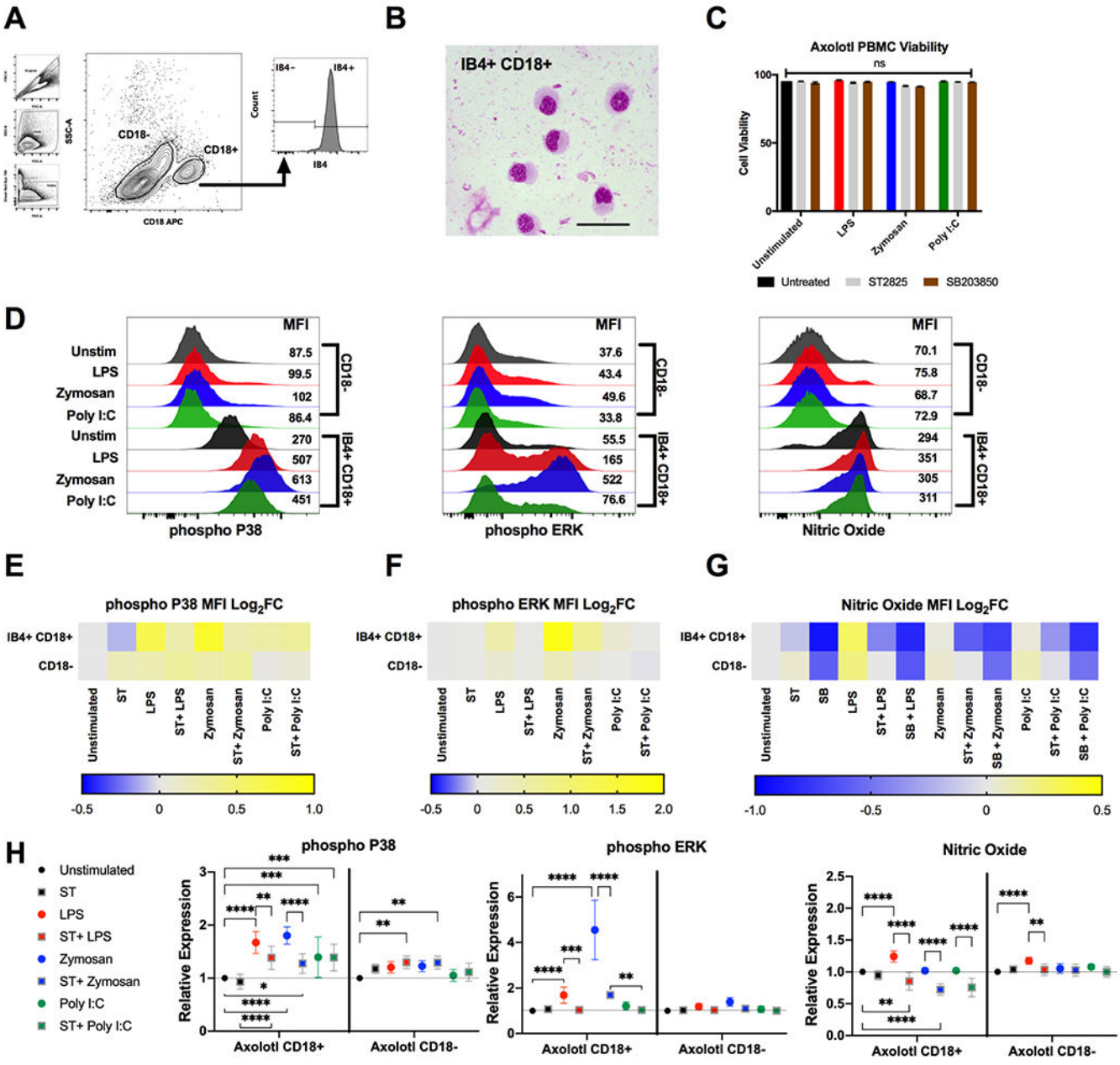

Figure 4. Conserved MyD88 dependent TLR induced MAPK signalling in axolotl PBMCs.

(A) Representative flow cytometry plot of gating strategy identifying viable monocytes using IB4 and CD18 in fixed/permeabilized PBMC samples. **(B)** Modified Giemsa-Wright stain of FACS isolated IB4+ CD18+ monocytes. Scale bars represent 50 μM. **(C)** Total cell viability as measured by Ghost Dye Red 780™ following stimulation with TLR2-4 agonists for 10 minutes. Grey bars represent samples treated with 50 μM ST2825 (MyD88 inhibitor), brown bars represent samples treated with 20 μM SB203850 (P38 MAPK inhibitor). (**D**) Representative flow cytometry histograms depicting the median fluorescent intensity (MFI) of IB4+ CD18+ and CD18− PBMCs for phospho-P38, phospho-ERK and nitric oxide (NO) following stimulation with 1 μg/mL LPS (red), 200 μg/mL zymosan A (blue) or 100 μg/mL

poly I:C (green) for 10 minutes. **(E-G)** Heat map depicting $\log_2$ fold changes of the average MFI of TLR stimulated and ST2825 or SB203850 treated samples n=8-12. Warmer colours indicate an increase in fold change whilst cooler colours indicate a decrease. **(H)** Relative stimulation/inhibition of each group showing statistically significant changes obtained via 2-way ANOVA Dunnet's test with multiple comparisons. **P ≤ 0.01, *** P ≤ 0.001 **** P ≤ 0.0001.

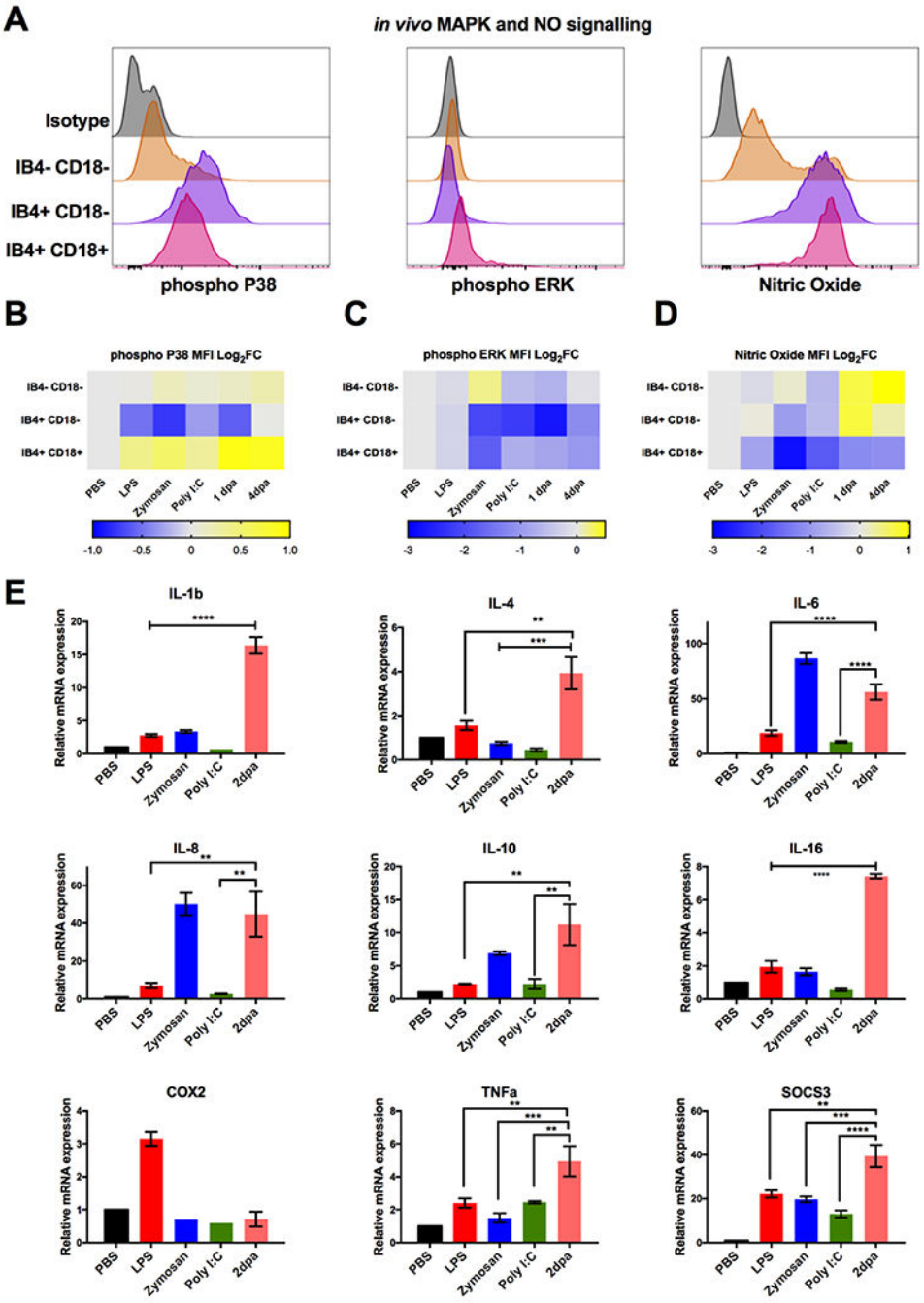

Figure 5. Regenerative tissues display unique inflammatory profiles compared with TLR stimulated tissues.

(A) Representative flow cytometry histograms depicting the expression of phospho-P38, phospho-ERK and nitric oxide in IB4+ CD18+, IB4+ CD18− and IB4− CD18− cells from limb tissue. **(B-D)** Heat map depicting $\log_2$ fold changes of the average median fluorescence intensity of IB4+ CD18+, IB4+ CD18− and IB4− CD18− cells during limb regeneration and *in vivo* TLR stimulation for **(B)** phospho-P38, **(C)** phospho-ERK and **(D)** nitric oxide. n=8. Warmer colours indicate an increase in fold change whilst cooler colours indicate a decrease.

(E) Comparison of inflammatory gene mRNA expression measured by quantitative RT-PCR. Bar charts represent mean ± SEM of 4 biological samples. p-values obtained via unpaired Student's t-test., **P ≤ 0.01, ***P ≤ 0.001 and ****P ≤ 0.0001.

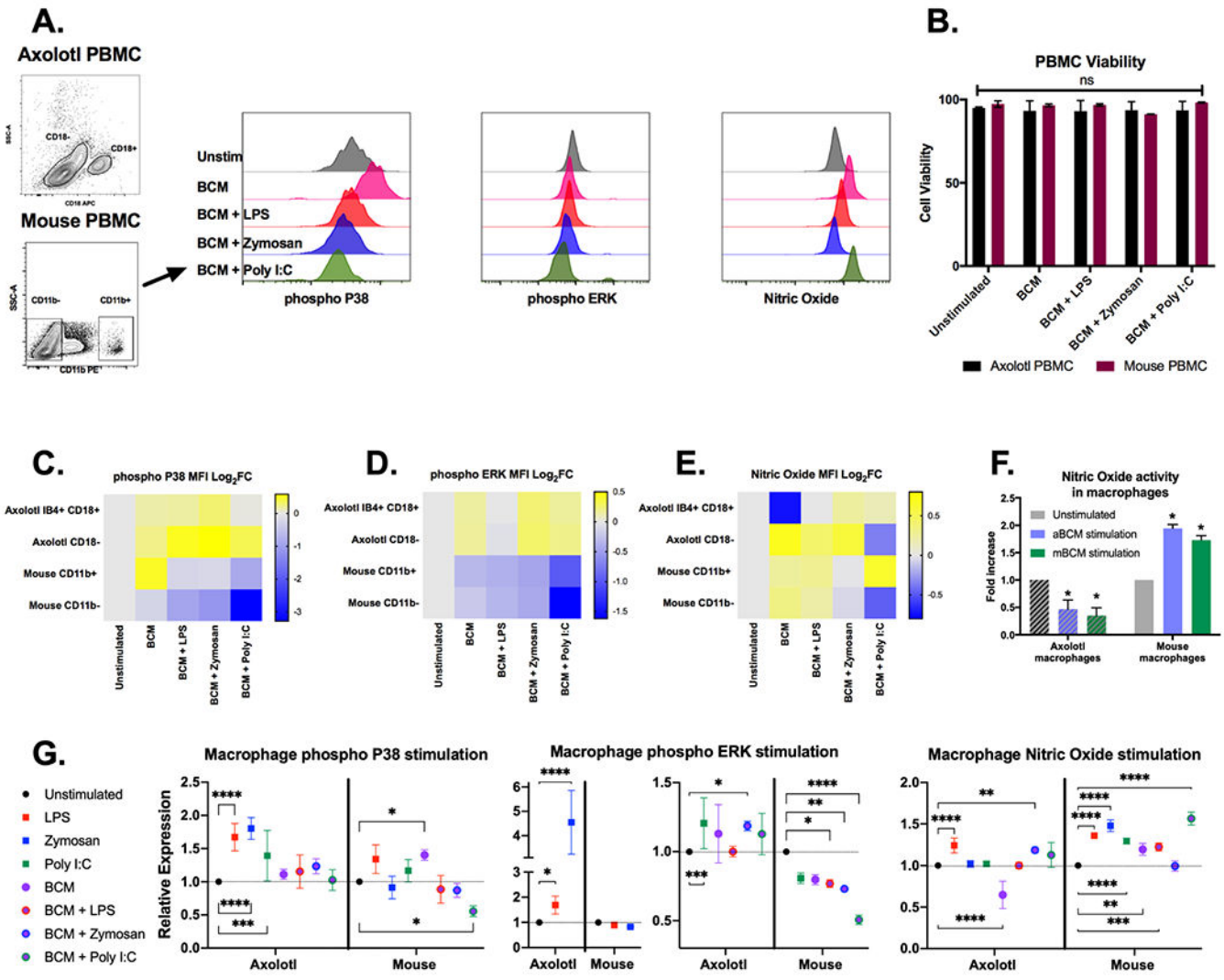

Figure 6. Rapid exposure to DAMP agonists induces immediate differential intracellular responses in mice and axolotls.

(A) Representative flow cytometry gating strategy to obtain phospho P38, phospho ERK and nitric oxide MFI values in mouse PBMCs following treatment with 200 μg/mL mouse BCM. BCM-TLR stimulation was performed for 10 minutes after which TLR-PAMP agonists (1 μg/mL LPS, 200 μg/mL zymosan A or 100 μg/mL poly I:C) were added for an extra 5 minutes. **(B)** Total cell viability as measured by Ghost Dye Red 780™ following TLR stimulation in axolotl (black bars) and mouse (dark red bars) PBMCs. **(C-E)** Heat map depicting $\log_2$ fold changes of the average MFI of TLR stimulated treated samples in axolotl and mouse PBMCs n=4. Warmer colours indicate an increase in fold change whilst cooler colours indicate a decrease. **(F)**. Reciprocal experiments reveal the profile of Nitric Oxide stimulation to be an intrinsic property of macrophages independent of donor BCM species. **(G)** Relative stimulation/inhibition of each group showing statistically significant changes obtained via 2-way ANOVA Dunnet's test with multiple comparisons. **P ≤ 0.01, *** P ≤ 0.001 **** P ≤ 0.0001.

Methods Table 1 –

Primers for qPCR analysis

Primer	Sequence
AxRBL27_F	CATCAGATCAAGCAAGCAGTA
AxRBL27_R	CCAATGCAGCAGTTTAGATG
AxBetaActin_F	TCCATGAAGGCTGCCCAACT
AxBetaActin_R	TGGCGCCACATCTGATTGAT
AxGAPDH_F	GACAAGGCATCTGCTCACCT
AxGAPDH_R	ATGTTCTGGTTGGCACCTCT
AxTLR2_F	AGAGTGGCCCTGCTGTAGAA
AxTLR2_R	TCTCCCTGATGGAGGAACAG
AxTLR3_F	CCCAGAAGCAAATGCTGAAT
AxTLR3_R	AACAGCCTGCATGAAACTCC
AxTLR4_F	GGAAACACATTTGGGGACAA
AxTLR4_R	GGCTACAACCAGAAATGTCCA
AxHMGB1_F	AGAGCGACAAGCAACGCTAT
AxHMGB1_R	GTTGAGGCCTGTACGAGGAG
AxIL1B_F	CGCCGCCCACAGCAGACATCC
AxIL1B_R	GGGCAGGCGGCTGACTCGAA
AxIL4_F	CGGCAGTATGCGTCAGAGT
AxIL4_R	CCGTTTCAGGGTCATTTTCA
AxIL6_F	CAAGCAGGGATTCAGAAAGG
AxIL6_R	AGAGCCAGCAGGAGTTCTGT
AxIL8_F	CCAAGCAAATTCGGACTGTT
AxIL8_R	CGTCCGATGTTCCTCATTGT
AxIL10_F	GAACAAGGACATCAGCAACG
AxIL10_R	CCCCTTATCCTGCATCTTGA
AxIL16_F	CTCAGTCATCGGGGTCATCT
AxIL16_R	CACCTTCCTCCTTGTGGAGA
AxCOX2_F	AACTCCTCCAGCTCTTGCGCCAT
AxCOX2_R	TCACAAATCAGCATGCAGGCCA
AxTNF-a_F	GAAGACATCACCCGAAGAGAGT
AxTNF-a_R	GGTTCCTGGTATCGGAAATATG
AxSOCS3_F	CTGACCACCACCACCTCTTT
AxSOCS3_R	CACAGATTGGTGTCCGATTG

Methods Table 2 –

Antibodies/reagents for flow cytometry/western blotting

Antibody/reagent	Clone	Application	Supplier (cat#)
Isolectin GS-B4 Biotin	N/A	FC (1 in 50)	Vector Labs (B-1205)
CD18 APC	Mouse mAb TS1/18	FC (1 in 50)	Biolegend (302114)
CD11b PE	Rat mAB M1/70	FC (1 in 400)	Biolegend (101208)
p-P38	Mouse mAB 28B10	FC (1 in 1500)	Cell Signalling Technology (9216L)
p-ERK	Rabbit Polyclonal	FC (1 in 200)	Cell Signalling Technology (4370S)
Streptavidin 568	N/A	FC (1 in 1000)	Thermo Fisher (S112226)
Streptavidin PE-Cy7	N/A	FC (1 in 1000)	Biolegend (405206)
Goat anti-mouse IgG (minimal x-reactivity) PE-Cy7	N/A	FC (1 in 1000)	Biolegend (405315)
Donkey anti-rabbit IgG Brilliant Violet 510	N/A	FC (1 in 300)	Biolegend (406419)
FC: flow cytometry			